Chemico-Biological Interactions 183 (2010) 341–348

Contents lists available at ScienceDirect

Chemico-Biological Interactions

journal homepage: www.elsevier.com/locate/chembioint

3-(4-(Benzo[d]thiazol-2-yl)-1-phenyl-1H-pyrazol-3-yl) phenyl acetate induced Hep G2 cell apoptosis through a ROS-mediated pathway

Jianyong Li[a], Zhijun Xu[b], Mengyao Tan[a], Weike Su[b], Xing-guo Gong[a,*]

[a] Institute of Biochemistry, College of Life Sciences, Zhejiang University, 310058, PR China
[b] Key Laboratory of Pharmaceutical Engineering of Ministry of Education, College of Pharmaceutical Sciences, Zhejiang University of Technology, Hangzhou, 310014, PR China

ARTICLE INFO

Article history:
Received 20 October 2009
Received in revised form 4 December 2009
Accepted 8 December 2009
Available online 16 December 2009

Keywords:
Benzothiazole
DPB-5
Apoptosis
ROS
Caspase

ABSTRACT

3-(4-(Benzo[d]thiazol-2-yl)-1-phenyl-1H-pyrazol-3-yl) phenyl acetate (DPB-5) is a synthetic benzothiazole derivative. In the present study, we revealed that DPB-5 had strong cytotoxicity to induce cell apoptosis, which was mediated by ROS. And DPB-5 was more cytotoxic toward hepatoma cells than toward normal hepatic cells, which was resulted from the greater susceptibility of the malignant cells to ROS. DBP-5 caused massive ROS accumulation and GSH decrease, which lead to MMP disruption, caspase activation and finally induced cell apoptosis. Additionally, rotenone, an inhibitor of mitochondria electron transport system, effectively blocked the ROS elevated effect of DPB-5, which suggested that DPB-5-induced ROS generated from the mitochondria. Further studies showed that DPB-5-induced cell apoptosis through caspases-cascade, but failed to activate caspase-9. Hence, we concluded that DPB-5-induced Hep G2 cells apoptosis via a ROS-mediated pathway which was caspase-dependent but did not rely on caspase-9.

1. Introduction

Apoptosis is important in chemotherapy-induced tumor-cell killing, and many anticancer drugs induce restoration of apoptosis [1–4]. Many tumors have been associated with the inhibition of apoptosis, and the disruption of apoptotic function which contribute substantially to the transformation of a normal cell into a tumor cell [5,6]. Intracellular reactive oxygen species (ROS) is considered to be a death signal in apoptosis [7–10]. ROS induces disruption of the mitochondrial membrane potential (MMP) and release of cytochrome c from mitochondria into the cytosol, where cytochrome c triggers caspase-9 activation and initiates caspases-cascade which terminates cell to apoptosis [11,12]. Accumulation of excessive ROS leads to lipid peroxidation, protein oxidation, enzyme inactivation, oxidative DNA damage [13,14]. Cancer cells are more sensitive to ROS than normal cells; therefore, ROS is considered as an important target for anticancer drug research [15,16].

Thiazole, an important heterocyclic ring, is widely used in anticancer drug development [17]. Many natural chemotherapeutic agents containing thiazole moiety have been discovered and studied, like tiazofurin [18,19], distamycin [20,21], bleomycin [22] and netropsin [21]. Among the thiazole derivatives, benzothiazole is an important scaffold of drugs, and it has been studied extensively. Benzothiazole derivatives are known as inhibitors of topoisomerase II, tyrosine kinase and ubiquitin–proteasome system [23–26]. Some studies reported the antioxidant properties of benzothiazole derivatives [27,28], and their biological activity was indicated to be strongly related to ROS [29]. In this respect, we examined the relationship between cytotoxic effect of 3-(4-(benzo[d]thiazol-2-yl)-1-phenyl-1H-pyrazol-3-yl) phenyl acetate (DPB-5, Fig. 1B) and ROS. DPB-5 is screened from a series of compounds derived from 2-(1,3-diphenyl-1H-pyrazol-4-yl) benzo[d]thiazole (DPB, Fig. 1A), which were designed and synthesized in earlier work.

In this study, we determined that DPB-5 had a strong specific cytotoxicity against Hep G2 cells, which was caused by apoptosis through a ROS-mediated pathway. DPB-5-induced cell death was caspase-dependent, but independent on caspase-9.

2. Materials and methods

2.1. Cell culture and reagent

Human cancer cell lines specific for: breast, MCF-7; hepatoma, Hep G2; laryngeal epithelium, Hep 2; gastric carcinoma, SGC 7901;

Abbreviations: DPB-5, 3-(4-(benzo[d]thiazol-2-yl)-1-phenyl-1H-pyrazol-3-yl) phenyl acetate; MTT, 3-(4,5-dimethylthiazol-2-yl)-2,5-diphenyltetrazolium bromide; ROS, reactive oxygen species; MMP, mitochondrial membrane potential; GSH, reduced glutathione; PI, propidium iodide; ROT, rotenone; DCFH-DA, dichlorodihydrofluorescein diacetate; NAC, N-acetyl-L-cysteine; Rh123, rhodamine 123; CAT, catalase; AMBAN, 2-acetyl-3-(6-methoxybenzothiazo)-2-yl-aminoacrylonitrile.

* Corresponding author at: Institute of Biochemistry, College of Life Sciences, Zhejiang University, Hangzhou, Zhejiang Province, 310058, PR China. Tel.: +86 571 88206475; fax: +86 571 88206549.
E-mail address: gongxingguo@126.com (X.-g. Gong).

0009-2797/$ – see front matter © 2009 Elsevier Ireland Ltd. All rights reserved.
doi:10.1016/j.cbi.2009.12.008

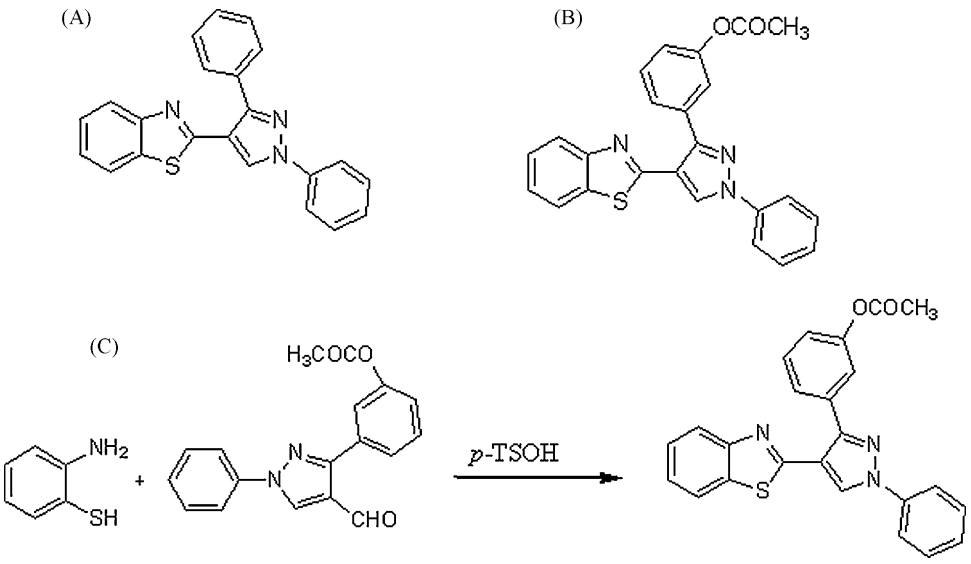

Fig. 1. Chemical structures and reaction. (A) Chemical structures of DPB; (B) chemical structures of DPB-5; (C) reaction for DPB-5 synthesized.

and leukaemia, HL60; were obtained from the Institute of Biochemistry and Cell Biology (Chinese Academy of Sciences). The human normal embryonic hepatic cell line LO2 was purchased from Nanjing KeyGen Biotech. Co. Ltd. (Nanjing, China). All cells used in this study were cultured at 37 °C in RPMI-1640 medium (Gibco) supplemented with 10% (v/v) fetal bovine serum (Gibco), 100 U/ml penicillin (Sigma) and 100 mg/ml streptomycin (Sigma), in a humidified 5% (v/v) CO_2 atmosphere. For the drug treatment experiments, cells were harvested during the exponential growth phase and seeded for 12–24 h, then the medium was replaced by RPMI-1640 medium supplemented with 2% FBS and containing various doses of drug, and kept incubation for further study.

DPB-5 was synthesized as in Fig. 1C, and purified by silica gel column chromatography. The purity was determined by TLC, and the structure determined by MS, ^{1}H NMR and ^{13}C NMR.

DPB-5, white solid. ^{1}H NMR (500 MHz, $CDCl_3$) δ: 2.29 (s, 3H), 7.23 (t, 1H, J = 8.0 Hz), 7.32–7.36 (m, 2H), 7.45–7.50 (m, 4H), 7.59 (s, 1H), 7.66 (d, 1H, J = 7.5 Hz), 7.80 (t, 4H, J = 8.0 Hz), 8.01 (d, 1H, J = 8.0 Hz), 8.60 (s, 1H). ^{13}C NMR (125 MHz, $CDCl_3$) 169.24, 159.77, 153.27, 150.84, 150.72 139.28, 135.03, 133.47, 129.61, 129.39, 128.53, 127.38, 127.07, 126.24, 124.95, 122.80, 122.69, 122.27, 121.45, 119.33, 117.32, and 21.19.

DPB-5 was dissolved in DMSO (Sigma) and diluted to the desired concentration before used, with the concentration of DMSO kept below 0.1% in the treatment groups. 3-(4,5-Dimethylthiazol-2-yl)-2,5-diphenyltetrazolium bromide (MTT), rhodamine 123 (Rh123), dichlorodihydrofluorescein diacetate (DCFH-DA), *N*-acetylcysteine (NAC), catalase (CAT), propidium iodide (PI) and rotenone (ROT) were purchased from Sigma. Naphthalene-2,3-dicarboxyaldehyde (NDA) was purchased from Molecular Probes. All other chemicals were analytical grade.

2.2. Cell viability assay

Cell viability was measured by the MTT assay method [30]. Briefly, cells in exponential growth phase were trypsinized, counted, and seeded in 96-well culture plates at a concentration of 5×10^3 cells/well. After cultured for 12 h, the medium was replaced by RPMI-1640 medium supplemented with 2% FBS containing various doses of drug. After incubation for the length of time indicated, MTT was added (final concentration 0.5 mg/ml) and kept incubating for 4 h. The formazan crystals were dissolved in 150 μl of DMSO and the plates were read at 570 nm with a microplate reader (model ELX800, Bio-Tek Instruments). The IC_{50}, calculated from 50% formazan formation compared with the control without drug treatment, were determined graphically using the curve-fit algorithm of the software PrismTM 2.0 (Graph-Pad). Each test was performed in triplicate.

2.3. Trypan blue exclusion

The cell death rate was determined by trypan blue exclusion method [31]. Cells in the exponential growth phase were plated at 5×10^4 cells/well in 24-wells culture plates. After 12 h growth, the medium was replaced by RPMI-1640 medium supplemented with 2% FBS containing various doses of DPB-5. After incubating for the indicated times, the viable cells and dead cells were counted on optical microscope with hemacytometer. Living cells possess intact cell membranes that exclude trypan blue dyes; however dead cells take up dyes and turn to blue. (Cell death %) = (total number of dead cells per ml of aliquot)/(total number of cells per ml of aliquot) × 100%.

2.4. Evaluation of apoptosis

2.4.1. Analysis of DNA fragmentation

Cells were treated with 15 μM DPB-5 for different lengths of time, harvested by centrifugation and washed twice in ice-cold PBS. An Apoptotic DNA Laddering Kit (Beyotime Institute of Biotechnology, China) was used to analyze DNA fragmentation according to the manufacturer's protocol, and then the DNA fragments in the samples were separated by electrophoresis in 1.8% (w/v) agarose gel.

2.4.2. Hoechst 33258 staining

Cells were seeded onto a glass slide and treated with 15 μM DPB-5 for 24 h, then washed twice with ice-cold PBS and fixed with 4% (v/v) formaldehyde in PBS for 20 min, washed with PBS, stained with 1 mg/ml Hoechst 33258 in PBS at 37 °C for 15 min, and then viewed under a fluorescence microscope (Nikon) with an excitation wavelength of 345 nm through the filter of 420 nm.

2.4.3. Annexin V-FITC/PI staining

Apoptosis was determined by translocation of phosphatidylserine to the cell surface using an Annexin V-FITC apoptosis detection kit (Nanjing KeyGen Biotech. Co. Ltd., China) according to the man-

ufacturer's protocol. Briefly, after treatment with DPB-5 for 48 h, cells were harvested and washed twice with ice-cold PBS, then evaluated for apoptosis using a FACSCalibur flow cytometer (BD Biosciences) with Annexin V–FITC and PI double staining. Fluorescence was measured with an excitation wavelength of 480 nm through FL-1 filter (530 nm) and FL-2 filter (585 nm).

2.4.4. Cell cycle analysis

Cells were treated with 8 μM or 15 μM DPB-5 for 48 h. The cells were harvested and washed twice with PBS, then fixed in ice-cold 70% (v/v) ethanol for 24 h at 4 °C. Before analysis, cells were washed with PBS, suspended in 1 ml of cold PI solution (50 μg/ml PI, 1% (v/v) Triton X-100, 100 μg/ml RNase A) and incubated on ice for 30 min in darkness. Cytometric analysis was performed using flow cytometer and Cell Quest software. Fluorescence was measured with an excitation wavelength of 480 nm through FL-2 filter. Apoptotic cells were detected on a PI histogram as a Pro G1 peak.

2.5. Measurement of mitochondrial membrane potential (MMP)

MMP was measured by flow cytometer using the cationic lipophilic green fluorochrome Rh123 [10]. Cells were harvested, washed twice with PBS, incubated with 1 μM Rh123 at 37 °C for 30 min, and washed twice with PBS. Fluorescence was determined by flow cytometer with an excitation wavelength of 480 nm at FL-1 filter.

2.6. Determination of cellular reactive oxygen species (ROS) and intracellular glutathione levels (GSH)

Intercellular ROS was determined by flow cytometer and staining with DCFH-DA. DCFH-DA is deacetylated by intracellular esterase and converted to nonfluorescent dichlorodihydrofluorescein, which is oxidized rapidly to the highly fluorescent compound dichlorofluorescein (DCF) in the presence of ROS. Cellular ROS content was measured by incubating the cells with 10 μM DCFH-DA at 37 °C for 30 min. After incubation with the fluorochrome, cells were washed with PBS and analyzed immediately by flow cytometer through FL-1 filter with an excitation wavelength of 480 nm.

The cellular level of reduced glutathione (GSH), another index reflecting cellular reducing power, was measured by staining cells with NDA [32]. GSH is oxidized to oxidized glutathione (GSSG) under the stress of ROS. Cells were stained with 200 μM NDA at 37 °C for 30 min, the level of GSH was determined by measuring the fluorescence intensity by flow cytometer with the FL-1 filter and an excitation wavelength of 480 nm.

2.7. Caspase-9 activity assay

Caspase-9 activity was measured using colorimetric assay kits (KeyGen Biotech Co., Ltd., Nanjing, China) according to the manufacturer's instructions. Briefly, cells treated with DPB-5 were harvested and lysed, then the lysate was incubated at 37 °C for 2 h with 200 μM LEHD-pNA (caspase-9 substrate). Samples were read at 405 nm in a microplate reader (Bio-Tek Instruments). Protein concentration was determined by Lowry method [33].

2.8. Statistical analysis

Unless otherwise stated, data are reported as mean ± SD. Comparisons between multiple treatments were made with analysis of variance (ANOVA) whereas comparisons between two treatments were made using a Student's *t*-test with $P \leq 0.05$ considered statistically significant.

Table 1
Effects of DPB-5 on the growth of human tumor cell lines.

Cell line	IC_{50} (μM)
Hep G2	4.6 ± 1.0
MCF-7	6.4 ± 0.6
Hep 2	11.7 ± 1.3
HL 60	6.3 ± 0.8
LO2	9.6 ± 0.6
SCG7901	8.3 ± 1.2

Cells were cultured for 48 h and the IC_{50} values were calculated using non-linear regression analysis. The data shown represent as means ± SD of three-independent experiments.

3. Results

3.1. Cytotoxicity analysis

MTT analysis showed the cell toxicity of DPB-5 against six human cell lines (Table 1). The hepatoma cell line Hep G2 was the most sensitive to DPB-5-induced cell toxicity, with an IC_{50} of 4.6 μM, while the laryngeal epithelial cell line Hep 2 and the normal embryonic hepatic cell line LO2 had a level of resistance more than twice of that of Hep G2, with IC_{50} values of 11.7 and 9.6 μM, respectively. Because of the particular sensitivity of Hep G2 cell line, we chose Hep G2 and the corresponding normal hepatic cell LO2 for further study.

Next we examined the cytotoxicity of DPB-5 against Hep G2 for various lengths of time and doses. As shown in Fig. 2, DPB-5-induced Hep G2 cell death in a time- and dose-dependent manner.

3.2. DPB-5-induced apoptosis in Hep G2 cells

In order to identify whether DPB-5-induced cell death in apoptotic mode, we observed DPB-5-treated Hep G2 cells by staining with Hoechst 33258 (Fig. 3A), DNA fragment ladder (Fig. 3.B), staining with Annexin V-FITC (Fig. 3C), and Pro G1 analysis (Fig. 3D). Cells treated with 15 μM DPB-5 for 24 h then stained with Hoechst 33258 showed condensed nuclei and apoptotic bodies. Genomic DNA of cells treated with 15 μM DPB-5 for 24 and 48 h showed typical DNA fragment ladders. When cells were stained with both Annexin V-FITC and PI, the cell membrane showed PS externalization. Compared to the control, cells treated with 15 μM DPB-5 for 48 h had an increase in the percentage of early apoptotic cells (Annexin V positive but PI negative) from 1.2% to 42.4%, and of late apoptotic cells (Annexin V and PI double-positive cells) from 1.9% to 35.8%. Analysis of the cell cycle by flow cytometer showed the dose-

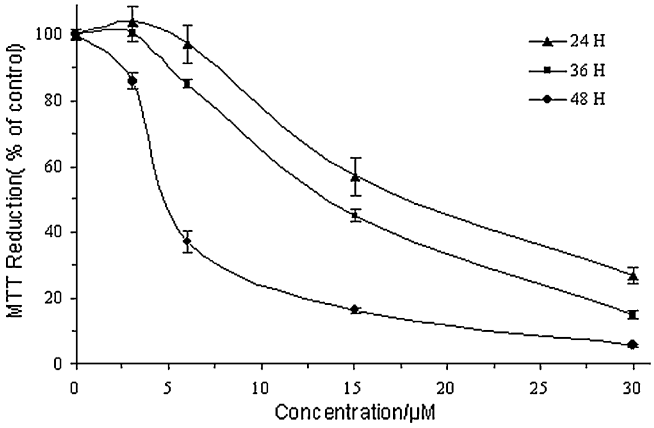

Fig. 2. Time- and dose-dependent effects of DPB-5 on Hep G2 cells. Cell viability was determined by a MTT assay as described in the text. Results are expressed as means ± SD of data obtained in three independent experiments.

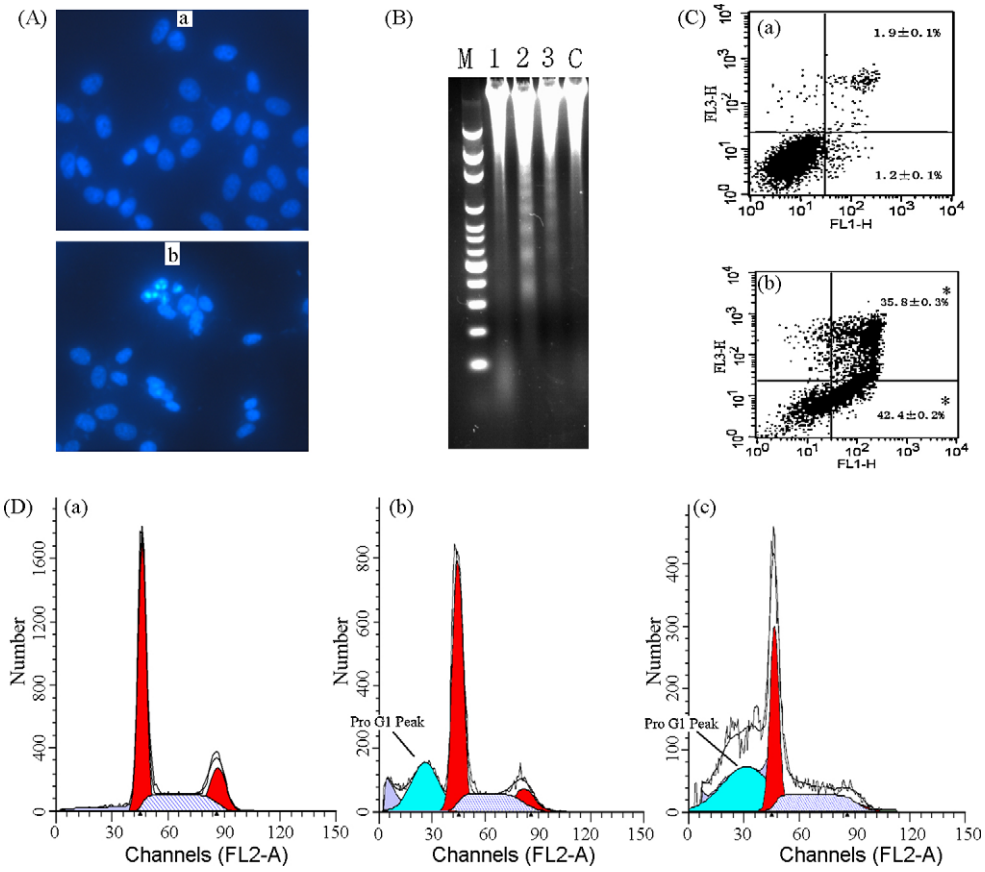

Fig. 3. Apoptotic effects of DPB-5 on Hep G2 cells. (A) Fluorescent microscopic analysis of apoptotic cells. Cells stained with Hoechst 33258 after treated with 15 μM DPB-5 for 24 h. (a) Control, (b) 15 μM DPB-5 for 24 h. (B) DNA fragmentation analysis for apoptosis. Hep G2 cells were pretreated with 15 μM DPB-5 for 24 and 48 h. M: marker, 1: 50 μM H_2O_2 for 6 h as positive control, 2: 15 μM DPB-5 for 48 h, 3: 15 μM DPB-5 for 24 h, C: control. (C) Annexin V-FITC and PI staining for apoptosis. Data were obtained in three separate experiments. (a) Control; (b) 15 μM DPB-5 for 48 h. (*$P \leqslant 0.05$ versus control) (D) Pro G1 analysis for apoptotic cells. Hypodiploid cells (apoptotic cells) are shown in region with green colour by ModFit LT software and marked as Pro G1 Peak. (a) Control; (b) 8 μM DPB-5 for 48 h; (c) 15 μM DPB-5 for 48 h. (For interpretation of the references to color in this figure legend, the reader is referred to the web version of the article.)

dependent increased Pro G1 peak. These results are all hallmarks of apoptotic cell death, and demonstrated the ability of DPB-5 to induce apoptosis in Hep G2 cells.

3.3. DPB-5-induced MMP disruption

It is generally agreed that MMP disruption irreversibly leads to cell death, resulting in mitochondrial release of apoptogenic factors and a decrease of ATP generation [4,34,35]. To gain a better understanding of the mechanism underlying DPB-5-induced apoptosis, we examined the effect of DPB-5 on MMP by examining the retention of Rh123. As shown in Fig. 4C, there was a time-dependent decrease of Rh123 fluorescence after treatment with DPB-5 compared with the untreated control, indicating that DPB-5-induced MMP disruption in Hep G2 cells. In contrast, normal cell LO2 was less sensitive to DPB-5.

3.4. DPB-5-induced ROS burst and GSH depletion

ROS and GSH are indices of cell redox status. The generation of intracellular ROS and depletion of GSH are always associated with MMP disruption and cell apoptosis [36,37]. Therefore, we examined the levels of ROS and GSH in Hep G2 cells and LO2 cells treated with DPB-5. ROS was monitored by the oxidation-sensitive fluorescent dye DCFH-DA. A time-dependent increase in DCF fluorescence was detected in DPB-5-treated cells (Fig. 4A). Rapid generation of ROS, up to 3.56-fold faster than the control, was detected only 2 h after drug treatment, while the fluorescence intensity was increased 10-fold after 12 h of drug treatment. However, DPB-5-induced less ROS change on LO2 cells with 1.5-fold after 12 h treatment compared to Hep G2 cells. We analyzed changes of the GSH level in Hep G2 cells and LO2 cells using NDA fluorescence. DPB-5 caused a significant decrease of the intracellular GSH content after 12 h of drug treatment compared to the less change on LO2 cells (Fig. 4B).

3.5. Antioxidants protected Hep G2 cell from DPB-5 cytotoxicity

To verify the relationship between ROS generation and cell toxicity, we examined the effects of ROS scavengers, NAC (a well-known antioxidant and GSH precursor) and catalase (CAT, a H_2O_2-scavenging enzyme), on DPB-5-induced cell death. Before treated with drugs, the cells were treated with 1 mM NAC or 2000 U/ml catalase for 30 min, and then the change of MMP and cell toxicity were determined. As shown in Fig. 5, both NAC and catalase inhibited the loss of MMP and protected cells from DPB-5 cytotoxicity. Further they both significantly reduced DPB-5-induced cell apoptosis as indicated by Hoechst staining and trypan blue exclusion. It is suggested that ROS accumulation caused MMP disruption and mediated cell apoptosis.

3.6. ROS generation that triggered by DPB-5 against Hep G2 originated from mitochondria

We identified and clarified the source of DPB-5-induced ROS burst in Hep G2 cells (Fig. 6). Mitochondria are considered to be

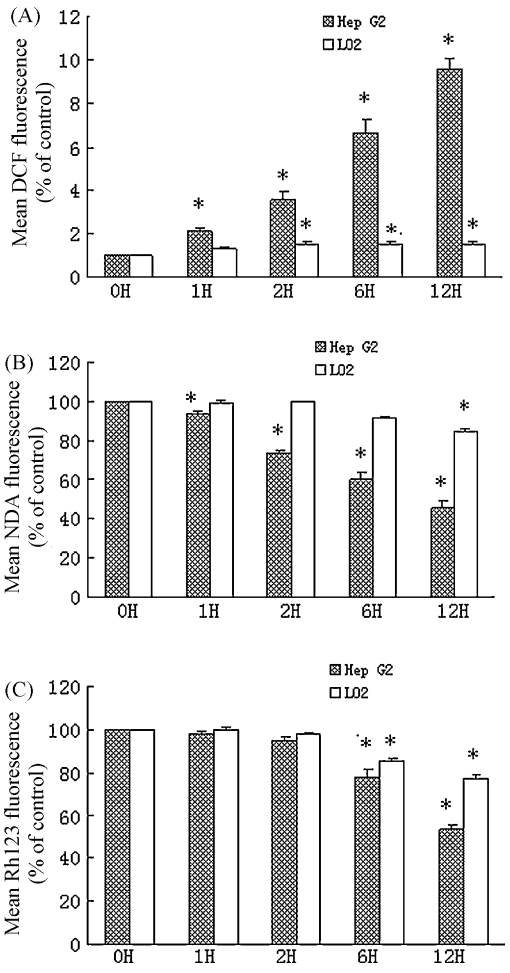

Fig. 4. DPB-5-induced ROS generation, GSH depletion and mitochondria membrane potential (MMP) disruption. (A) Effect of DPB-5 on cellular ROS production. After treatment with 10 μM DPB-5 for 0–12 h, cells were incubated with 10 μM DCFH-DA for 30 min and then immediately subjected to flow-cytometric analysis. Results are expressed as a ratio of relative fluorescent intensity compared to the control group. (B) Effect of DPB-5 on cellular GSH level. Cellular GSH level was examined by flow-cytometric analysis as describe in text after treated with 10 μM DPB-5 for 0–12 h. Results are expressed as a percentage of relative fluorescent intensity compared to the control group. (C) Effect of DPB-5 on MMP. After treated with 10 μM DPB-5 for 0–12 h, cells determined by flow-cytometric analysis stained with Rho 123 for 30 min. Results are expressed as a percentage of relative fluorescent intensity compared to the control group. The data represent means ± SD of three independent experiments; $^{*}P \leqslant 0.05$ versus control.

the main source of ROS in most tumor cells [38]. It is estimated that about 2% of the oxygen in a cell leaks from the mitochondrial electron transport chain and becomes ROS under physiological condition [39]. We investigated the effect of rotenone (ROT, an inhibitor of mitochondrial electron transport chain complex I) on DPB-5-induced ROS generation. Hep G2 cells were treated with 5 μM rotenone for 30 min, and then treated with or without 10 μM DPB-5 for 2 h. Compared with the 2.56-fold increase without any pretreatment, the treatment with rotenone blocked the DPB-5-induced ROS generation significantly (Fig. 6). This result suggested that DPB-5 triggered the generation of ROS by the mitochondria.

3.7. DPB-5-induced cell apoptosis in a caspase-dependent pathway but not caspase-9 dependent

Caspases play a critical role in the process of cell apoptosis [40]. Caspase-9 is a major mediator of apoptosis. Surprisingly, DPB-5 failed to activate caspase-9 while H_2O_2, as a positive control, significantly increased its activity. However as the cells pretreated with zVADfmk (a synthetic pan-caspase inhibitor, purchased from Promega) to inhibit the caspase activity, the cell death rate was massively reduced and cell apoptosis was significantly inhibited (Fig. 7). It is suggested that DPB-5-induced cell apoptosis in a caspase-dependent pathway but not depend on caspase-9.

4. Discussion

In this study, Hep G2 cells were shown to be much more sensitive to DPB-5-induced cytotoxicity than four other tumor cells and LO2 normal cells; and the DPB-5-induced Hep G2 cell death was both dose- and time-dependent. The cytotoxic effect of DPB-5 caused apoptotic cell death, as determined by DNA fragmentation, morphological change of the nucleus, increase of pro-G1 DNA content, and externalization of phosphatidylserine.

ROS plays an important role in apoptosis. The apoptotic effect of DPB-5 on Hep G2 cells was associated with an early elevated level of intracellular ROS. After treatment with DPB-5 for 1 h, ROS was increased to 2.56-fold, and continued to increase with time, reaching almost 10-fold after 12 h treatment. However, the ROS change to normal cells LO2 was not so significant with only 0.5-fold increase after 12 h. In conjunction, the ROS generation was supported by the significant decrease of intercellular GSH, a main non-protein antioxidant in the cell, which is able to clear intracellular ROS [41] and inversely proportional to ROS level [42]. Consistent with continuous ROS generation, our result indicated that DPB-5-induced significant reduction of intracellular GSH on Hep G2 cells, while less change on LO2 cells. The higher vulnerability to ROS of Hep G2 cells than LO2 cells lead to the higher cytotoxicity of Hep G2 cells on DPB-5 than that of LO2 cells. Cancer cells, function with a heightened basal level of ROS-mediated signal, which is required for the increased rate of growth, may be more vulnerable to oxidant stress. A further oxidative stress could exhaust the cellular antioxidant capacity and push the ROS stress level beyond a "threshold", which would cause cell apoptosis [16].

Moreover, in order to confirm that the apoptotic effect of DPB-5 was mediated by ROS, antioxidants NAC and catalase were used. Both NAC and GSH inhibited the cytotoxicity of DPB-5 associated with suppressed ROS generation and GSH depletion. And they both can ensure cell survival as shown by trypan blue exclusion and significantly reduced cell apoptosis as demonstrated by Hoechst staining. Our results also indicated that DPB-5 induced a decrease of MMP in Hep G2 cells. In addition, concerning the time course of ROS burst and MMP depolarization, the ROS burst occurred before intracellular MMP depolarization. This opinion was supported by the results obtained from Hep G2 co-incubated with DPB-5 and antioxidant NAC or catalase. Both NAC and catalase blocked the MMP depolarization completely. These results demonstrated that the ROS burst was a prerequisite for MMP collapse and cell death induced by DPB-5.

In addition, we also determined that DPB-5-induced ROS production by the mitochondria. When inhibiting the cell respiration by rotenone (an inhibitor of the mitochondrial electron transport chain complex I), the DPB-5-induced generation of ROS in Hep G2 cells was blocked completely. It is well accepted that ROS is generated from ETC primarily in the form of the superoxide anion (O_2^-), which is quickly transformed to hydrogen peroxide (H_2O_2), a stable form of ROS. In our study, however, O_2^- in Hep G2 cells treated with DPB-5 showed no significant change when stained with dihydroethidium (data not shown). Meanwhile, there was a dramatic increase of intracellular ROS (examined by DCFH-DA), which was generated by the mitochondria. We postulate that DPB-5-induced ROS generation is related to the mitochondrial protein $p66^{shc}$,

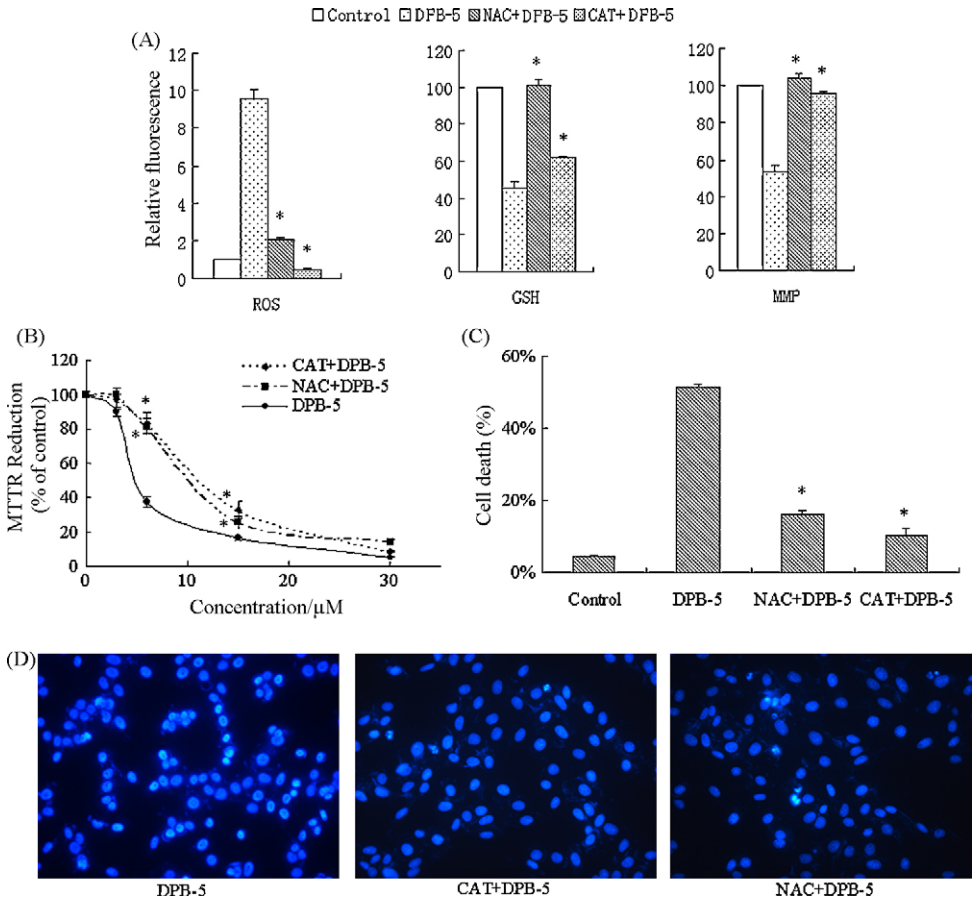

Fig. 5. Effects of exogenous application of NAC and catalase (CAT) on the DPB-5-induced ROS generation, GSH depletion MMP disruption, and cell viability of Hep G2 cells. (A) The ROS, GSH and MMP changes were examined by flow-cytometric analysis. (B) Cell viability was analyzed using MTT assay. Cells treated with DPB-5 for 48 h with or without pretreated with 1 mM NAC or 2000 U/ml catalase. (C) Cell death rate was determined by trypan blue exclusion. Control, cells treated with solvent as control; DPB-5, cells treated with 6 μM DPB-5 for 48 h; CAT+ DPB-5, cells treated with 6 μM DPB-5 for 48 h after incubated with 2000 U/ml catalase for 30 min; NAC + DPB-5, cells treated with 6 μM DPB-5 for 48 h after incubated with 1 mM NAC for 30 min. (D) catalase and NAC protected cells from apoptotic effect of DPB-5 determined by Hoechst staining. DPB-5: cells treated with 6 μM DPB-5 for 36 h; CAT+ DPB-5: cells treated with 6 μM DPB-5 for 36 h after pretreated with 2000 U/ml catalase for 30 min; NAC + DPB-5: cells treated with 6 μM DPB-5 for 36 h after pretreated with 1 mM NAC for 30 min. (The data represent means ± SD of three independent experiments; $^*P \leqslant 0.05$, cells treated with DPB-5 after incubated with NAC or catalase were compared with cells treated with DPB-5 alone.)

which acts downstream of ETC to oxidize reduced cytochrome *c*, generating H_2O_2 directly without O_2^- [43]. Further, $p66^{shc}$ acts as a regulator of mitochondrial metabolism, so the small increase of MTT reduction induced in a short time by a low concentration of DPB-5 (Fig. 2) may be related to the increase of cell mitochondrial metabolism induced by the activation of $p66^{shc}$ [44].

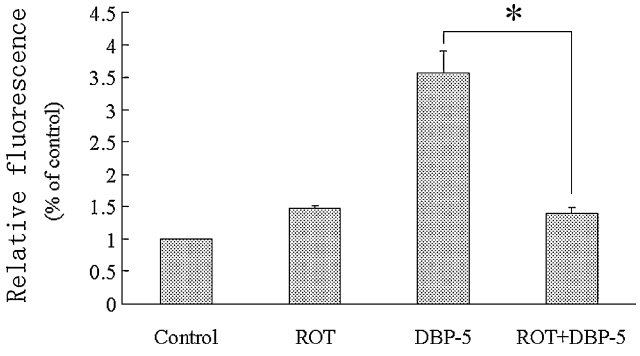

Fig. 6. Effect of rotenone (ROT) on the ROS induced by DPB-5. ROS level was analyzed using flow-cytometric analysis stained with DCFH-DA. Cells co-treated with DPB-5 for 2 h after pretreated with 5 μM rotenone for 30 min. (The data represents the means ± SD of three independent experiments with triplicates. $^*P < 0.05$ compared to DPB-5 alone group.)

The caspases-cascade system plays crucial roles in cell apoptosis. It is reported that caspases are the executors of apoptosis. Benzothiazole containing phthalimide induced human hepatoma cell SKHep1 and Burkitt's lymphoma cell CA46 apoptosis in both caspase-dependent and caspase-independent pathways [45], while 2-acetyl-3-(6-methoxybenzothiazo)-2-yl-aminoacrylonitrile (AMBAN) induced human leukemia cells HL60 and U937 apoptosis through a caspase-dependent pathway [29]. In the present paper, caspases played a critical role in DPB-5-induced cell death. When preincubated with pan-caspase inhibitor zVADfmk, the apoptotic effect of DPB-5 was significantly inhibited and the death rate was obviously reduced. AMBAN induced ROS increase as a death signal, which is similar to DPB-5. AMBAN decreased the mitochondrial membrane potential, released cytochrome *c*, and then activated caspase-9 to initiate caspases-cascade, which finally lead to cell apoptosis. Surprisingly, different from AMBAN, DPB-5 neither increased nor reduced the activity of caspase-9. It is supposed that other initiator caspases could be recruited and activated caspases-cascade.

In conclusion, the apoptotic effect of DPB-5 is mediated by ROS and relied on caspases-cascade. DPB-5 exerts higher cytotoxicity to Hep G2 cells than normal liver cells LO2, which is resulted from the vulnerability of cancer cells to ROS. Moreover this selective cytotoxic effect to Hep G2 suggested the anticancer potential of DPB-5.

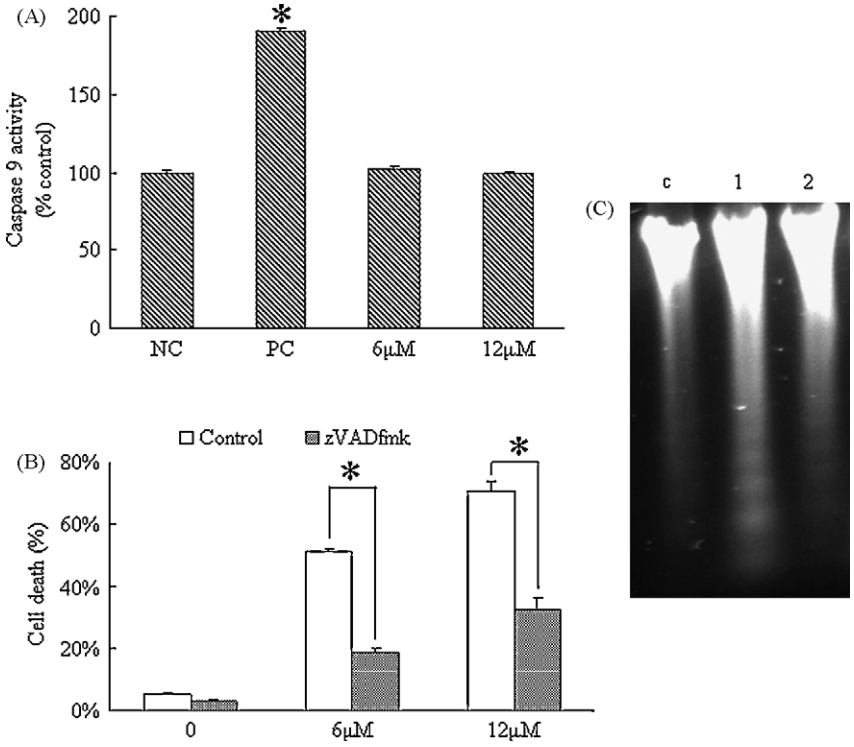

Fig. 7. DPB-5-induced Hep G2 cells apoptosis in a caspase-dependent pathway but independent on caspase-9. (A) Change of caspase-9 activity after treated with 6 μM or 12 μM of DPB-5 12 h. NC: negative control; PC: positive control, 50 μM H_2O_2 treated for 6 h. ($^*P \leqslant 0.05$ compared with control.) (B) Pan-caspase inhibitor zVADfmk protected cells death induced by DPB-5. Cell death rate after 48 h DPB-5 treatment with or without zVADfmk pretreated, which was determined by trypan blue exclusion as described in text. Control, cells treated with DPB-5 as control; zVADfmk, cells treated with DPB-5 after incubated 20 μM zVADfmk for 30 min. (The data represent means ± SD of three independent experiments; $^*P \leqslant 0.05$ compared with DPB-5 alone group.) (C) zVADfmk inhibits DPB-5-induced cell apoptosis showed by DNA fragment analysis. c: control, cells treated with solvent as control; 1: cells treated with 6 μM DPB-5 for 36 h; 2: cells which pretreated with 20 μM zVADfmk for 30 min treated with 6 μM DPB-5 for 36 h.

Conflict of interest statement

The authors declare that they have no competing interests.

Acknowledgment

This work was supported by a grant from the Key Science and Technique Programs of Zhejiang Province (No. 2006c12084).

References

[1] Y. Qin, F.D. Chen, L. Zhou, X.G. Gong, Q.F. Han, Proliferative and anti-proliferative effects of thymosin alpha1 on cells are associated with manipulation of cellular ROS levels, Chem. Biol. Interact. 180 (2009) 383–388.
[2] B. Fadeel, S. Orrenius, B. Zhivotovsky, Apoptosis in human disease: a new skin for the old ceremony? Biochem. Biophys. Res. Commun. 266 (1999) 699–717.
[3] C.B. Thompson, Apoptosis in the pathogenesis and treatment of disease, Science 267 (1995) 1456–1462.
[4] W. Hu, J.J. Kavanagh, Anticancer therapy targeting the apoptotic pathway, Lancet Oncol. 4 (2003) 721–729.
[5] J. Rohayem, P. Diestelkoetter, B. Weigle, A. Oehmichen, M. Schmitz, J. Mehlhorn, K. Conrad, E.P. Rieber, Antibody response to the tumor-associated inhibitor of apoptosis protein survivin in cancer patients, Cancer Res. 60 (2000) 1815–1817.
[6] E.C. LaCasse, S. Baird, R.G. Korneluk, A.E. MacKenzie, The inhibitors of apoptosis (IAPs) and their emerging role in cancer, Oncogene 17 (1998) 3247–3259.
[7] G.A. Murrell, M.J. Francis, L. Bromley, Modulation of fibroblast proliferation by oxygen free radicals, Biochem. J. 265 (1990) 659–665.
[8] T.M. Buttke, P.A. Sandstrom, Oxidative stress as a mediator of apoptosis, Immunol. Today 15 (1994) 7–10.
[9] K.R. Martin, J.C. Barrett, Reactive oxygen species as double-edged swords in cellular processes: low-dose cell signaling versus high-dose toxicity, Hum. Exp. Toxicol. 21 (2002) 71–75.
[10] M. Lu, X. Gong, Y. Lu, J. Guo, C. Wang, Y. Pan, Molecular cloning and functional characterization of a cell-permeable superoxide dismutase targeted to lung adenocarcinoma cells. Inhibition cell proliferation through the Akt/p27kip1 pathway, J. Biol. Chem. 281 (2006) 13620–13627.
[11] D.R. Green, J.C. Reed, Mitochondria and apoptosis, Science 281 (1998) 1309–1312.
[12] H.U. Simon, A. Haj-Yehia, F. Levi-Schaffer, Role of reactive oxygen species (ROS) in apoptosis induction, Apoptosis 5 (2000) 415–418.
[13] R.J. Mallis, J.E. Buss, J.A. Thomas, Oxidative modification of H-ras: S-thiolation and S-nitrosylation of reactive cysteines, Biochem. J. 355 (2001) 145–153.
[14] B.N. Ames, Endogenous DNA damage as related to cancer and aging, Mutat. Res. 214 (1989) 41–46.
[15] P.T. Schumacker, Reactive oxygen species in cancer cells: live by the sword, die by the sword, Cancer Cell 10 (2006) 175–176.
[16] H. Pelicano, D. Carney, P. Huang, ROS stress in cancer cells and therapeutic implications, Drug Resist. Update 7 (2004) 97–110.
[17] M.S. Karthikeyan, Synthesis, analgesic, anti-inflammatory and antimicrobial studies of 2,4-dichloro-5-fluorophenyl containing thiazolotriazoles, Eur. J. Med. Chem. 44 (2009) 827–833.
[18] G.J. Tricot, H.N. Jayaram, E. Lapis, Y. Natsumeda, C.R. Nichols, P. Kneebone, N. Heerema, G. Weber, R. Hoffman, Biochemically directed therapy of leukemia with tiazofurin, a selective blocker of inosine 5′-phosphate dehydrogenase activity, Cancer Res. 49 (1989) 3696–3701.
[19] E. Olah, Y. Natsumeda, T. Ikegami, Z. Kote, M. Horanyi, J. Szelenyi, E. Paulik, T. Kremmer, S.R. Hollan, J. Sugar, et al., Induction of erythroid differentiation and modulation of gene expression by tiazofurin in K-562 leukemia cells, Proc. Natl. Acad. Sci. U.S.A. 85 (1988) 6533–6537.
[20] M. Coll, C.A. Frederick, A.H. Wang, A. Rich, A bifurcated hydrogen-bonded conformation in the d(A.T) base pairs of the DNA dodecamer d(CGCAAATTTGCG) and its complex with distamycin, Proc. Natl. Acad. Sci. U.S.A. 84 (1987) 8385–8389.
[21] M.L. Kopka, C. Yoon, D. Goodsell, P. Pjura, R.E. Dickerson, The molecular origin of DNA-drug specificity in netropsin and distamycin, Proc. Natl. Acad. Sci. U.S.A. 82 (1985) 1376–1380.
[22] L.H. Einhorn, J. Donohue, Cis-diamminedichloroplatinum, vinblastine, and bleomycin combination chemotherapy in disseminated testicular cancer, Ann. Intern. Med. 87 (1977) 293–298.
[23] P. Sharma, N. Ghoshal, Exploration of a binding mode of benzothiazol-2-yl acetonitrile pyrimidine core based derivatives as potent c-Jun N-terminal kinase-3 inhibitors and 3D-QSAR analyses, J. Chem. Inf. Model. 46 (2006) 1763–1774.
[24] P. Guedat, F. Colland, Patented small molecule inhibitors in the ubiquitin proteasome system, BMC Biochem. 8 (Suppl. 1) (2007) S14.
[25] S.J. Choi, H.J. Park, S.K. Lee, S.W. Kim, G. Han, H.Y. Choo, Solid phase combinatorial synthesis of benzothiazoles and evaluation of topoisomerase II inhibitory activity, Bioorg. Med. Chem. 14 (2006) 1229–1235.
[26] A. Pinar, P. Yurdakul, I. Yildiz, O. Temiz-Arpaci, N.L. Acan, E. Aki-Sener, I. Yalcin, Some fused heterocyclic compounds as eukaryotic topoisomerase II inhibitors, Biochem. Biophys. Res. Commun. 317 (2004) 670–674.

[27] C. Prouillac, P. Vicendo, J.C. Garrigues, R. Poteau, G. Rima, Evaluation of new thiadiazoles and benzothiazoles as potential radioprotectors: free radical scavenging activity in vitro and theoretical studies (QSAR, DFT), Free Radic. Biol. Med. 46 (2009) 1139–1148.
[28] O. Temiz-Arpaci, T. Coban, B. Tekiner-Gulbas, B. Can-Eke, I. Yildiz, E. Aki-Sener, I. Yalcin, M. Iscan, A study on the antioxidant activities of some new benzazole derivatives, Acta. Biol. Hung. 57 (2006) 201–209.
[29] A. Repicky, S. Jantova, L. Cipak, Apoptosis induced by 2-acetyl-3-(6-methoxybenzothiazo)-2-yl-amino-acrylonitrile in human leukemia cells involves ROS-mitochondrial mediated death signaling and activation of p38 MAPK, Cancer Lett. 277 (2009) 55–63.
[30] Y. Shi, C.H. Wang, X.G. Gong, Apoptosis-inducing effects of two anthraquinones from *Hedyotis diffusa* WILLD, Biol. Pharm. Bull. 31 (2008) 1075–1078.
[31] M.F. Mian, C. Kang, S. Lee, J.H. Choi, S.S. Bae, S.-H. Kim, Y.-H. Kim, S.H. Ryu, P.-G. Suh, J.-S. Kim, E. Kim, Cleavage of focal adhesion kinase is an early marker and modulator of oxidative stress-induced apoptosis, Chem. Biol. Interact. 171 (2008) 57–66.
[32] O. Orwar, H.A. Fishman, N.E. Ziv, R.H. Scheller, R.N. Zare, Use of 2,3-naphthalenedicarboxaldehyde derivatization for single-cell analysis of glutathione by capillary electrophoresis and histochemical localization by fluorescence microscopy, Anal. Chem. 67 (1995) 4261–4268.
[33] E.F. Hartree, Determination of protein: a modification of the Lowry method that gives a linear photometric response, Anal. Biochem. 48 (1972) 422–427.
[34] J.L. Scarlett, P.W. Sheard, G. Hughes, E.C. Ledgerwood, H.H. Ku, M.P. Murphy, Changes in mitochondrial membrane potential during staurosporine-induced apoptosis in Jurkat cells, FEBS Lett. 475 (2000) 267–272.
[35] J.D. Ly, D.R. Grubb, A. Lawen, The mitochondrial membrane potential (deltapsi(m)) in apoptosis; an update, Apoptosis 8 (2003) 115–128.
[36] Y. Xiong, X. Liu, C.P. Lee, B.H. Chua, Y.S. Ho, Attenuation of doxorubicin-induced contractile and mitochondrial dysfunction in mouse heart by cellular glutathione peroxidase, Free Radic. Biol. Med. 41 (2006) 46–55.
[37] E. Lopez, C. Arce, M.J. Oset-Gasque, S. Canadas, M.P. Gonzalez, Cadmium induces reactive oxygen species generation and lipid peroxidation in cortical neurons in culture, Free Radic. Biol. Med. 40 (2006) 940–951.
[38] T. Hennet, C. Richter, E. Peterhans, Tumour necrosis factor-alpha induces superoxide anion generation in mitochondria of L929 cells, Biochem. J. 289 (1993) 587–592.
[39] M. Inoue, E.F. Sato, M. Nishikawa, A.M. Park, Y. Kira, I. Imada, K. Utsumi, Mitochondrial generation of reactive oxygen species and its role in aerobic life, Curr. Med. Chem. 10 (2003) 2495–2505.
[40] Y. Shi, Mechanisms of caspase activation and inhibition during apoptosis, Mol. Cell 9 (2002) 459–470.
[41] S.G. Rhee, K.S. Yang, S.W. Kang, H.A. Woo, T.S. Chang, Controlled elimination of intracellular H(2)O(2): regulation of peroxyredoxin, catalase, and glutathione peroxidase via post-translational modification, Antioxid. Redox Signal. 7 (2005) 619–626.
[42] Y. Higuchi, Glutathione depletion-induced chromosomal DNA fragmentation associated with apoptosis and necrosis, J. Cell Mol. Med. 8 (2004) 455–464.
[43] M. Giorgio, E. Migliaccio, F. Orsini, D. Paolucci, M. Moroni, C. Contursi, G. Pelliccia, L. Luzi, S. Minucci, M. Marcaccio, P. Pinton, R. Rizzuto, P. Bernardi, F. Paolucci, P.G. Pelicci, Electron transfer between cytochrome c and p66Shc generates reactive oxygen species that trigger mitochondrial apoptosis, Cell 122 (2005) 221–233.
[44] S. Nemoto, C.A. Combs, S. French, B.H. Ahn, M.M. Fergusson, R.S. Balaban, T. Finkel, The mammalian longevity-associated gene product p66shc regulates mitochondrial metabolism, J. Biol. Chem. 281 (2006) 10555–10560.
[45] S.H. Kok, R. Gambari, C.H. Chui, M.C. Yuen, E. Lin, R.S. Wong, F.Y. Lau, G.Y. Cheng, W.S. Lam, S.H. Chan, K.H. Lam, C.H. Cheng, P.B. Lai, M.W. Yu, F. Cheung, J.C. Tang, A.S. Chan, Synthesis and anti-cancer activity of benzothiazole containing phthalimide on human carcinoma cell lines, Bioorg. Med. Chem. 16 (2008) 3626–3631.